

Probing Charge Separation in Structurally Different C₆₀/exTTF Ensembles

Marta C. Díaz, M^a Angeles Herranz, Beatriz M. Illescas, and Nazario Martín*

Departamento de Química Orgánica, Facultad de Ciencias Químicas, Universidad Complutense, E 28040 Madrid, Spain

Nicolas Godbert and Martin R. Bryce*

Department of Chemistry, University of Durham, South Road, Durham DH1 3LE, UK

Chuping Luo, Angela Swartz, Greg Anderson, and Dirk M. Guldi*

Radiation Laboratory, University of Notre Dame, Indiana 46556

nazmar@quim.ucm.es

Received April 4, 2003

The scope of the present work is to highlight the effects stemming from different C₆₀/exTTF linkages (exTTF = 9,10-bis(1,3-dithiol-2-ylidene)-9,10-dihydroanthracene)—either via an anthracene unit or a dithiole ring. Particular emphasis is placed on photoinduced electron-transfer features. Therefore, we devised a new series of C₆₀-exTTF ensembles, synthesized via 1,3-dipolar cycloaddition and Diels–Alder cycloaddition reactions, in which exTTF units are separated from C₆₀ by two single bonds (**3a–c**, **4**), one vinylene unit (**5a**), or two vinylene units (**5b**). The cyclic voltammetry reveals an amphoteric redox behavior with remarkably strong electron-donor ability of the trimethyl-substituted exTTF moiety in **4** and **5a,b**. Steady-state and time-resolved photolytic techniques show that the fullerene singlet excited state in (**3a–c**, **4**, and **5a,b**) is subject to a rapid electron-transfer quenching. The resulting charge-separated states, that is C₆₀^{•–}-exTTF^{•+}, were identified by transient absorption spectroscopy. We determined radical pair lifetimes of the order of 200 ns in benzonitrile. This suggests (i) that the positive charge of the exTTF^{•+} is delocalized over the entire donor rather than localized on one of the 1,3-dithiole rings and (ii) that linking exTTF via the anthracene or 1,3-dithiole ring has no appreciable influence. Increasing the donor–acceptor separation via implementing one or two vinylene units as spacers led to improved radical pair lifetimes (**5a**: τ = 725 ns; **5b**: τ = 1465 ns).

Introduction

In the past decade, fullerenes emerged as a molecular tecton ideally suited for devising multicomponent model systems to transmit and process solar energy. Thus, the design of novel fullerene derivatives currently constitutes an active research area toward artificial light harvesting antenna and reaction center mimics. In these model systems, the specific composition of electron donors linked to C₆₀ has been utilized to tune the electronic couplings between donor and acceptor sites.¹ Fullerenes are three-dimensional electron acceptor modules able to accept up to six electrons in solution.² On account of C₆₀'s small reorganization energy in electron-transfer reactions, it has exerted a noteworthy impact on the improvement of light-induced charge-separation.³

Tetrathiafulvalene (TTF) and especially *p*-quinonoid π -extended tetrathiafulvalenes (exTTFs) are strong electron donor molecules, which are oxidized at relatively low anodic potential values to form the respective π -radical cation (TTF^{•+}) and dication (TTF²⁺ and exTTF²⁺) species. All the oxidized species (i.e., TTF^{•+}, TTF²⁺, and exTTF²⁺) are thermodynamically stable products, a consequence that stems primarily from the aromatic character of the generated dithiolium cations.⁴

Thus, integration of TTF—a donor whose oxidized state is aromatic—and C₆₀—an acceptor that accelerates charge separation and decelerates charge recombination—into novel molecular donor–acceptor ensembles holds great expectations to ultimately improve light-induced charge-separation processes. Up to now, a wide variety of C₆₀-TTF⁵ and C₆₀-exTTF⁶ dyads as well as C₆₀/TTF and C₆₀/exTTF triads⁷ were designed and probed as artificial reaction centers. Most remarkably, the radical pair lifetimes found, when using TTF and exTTF donor moieties, turned out to be some of the longest values

* To whom correspondence should be addressed. Fax: +34-913944103. Phone: +34-913944227.

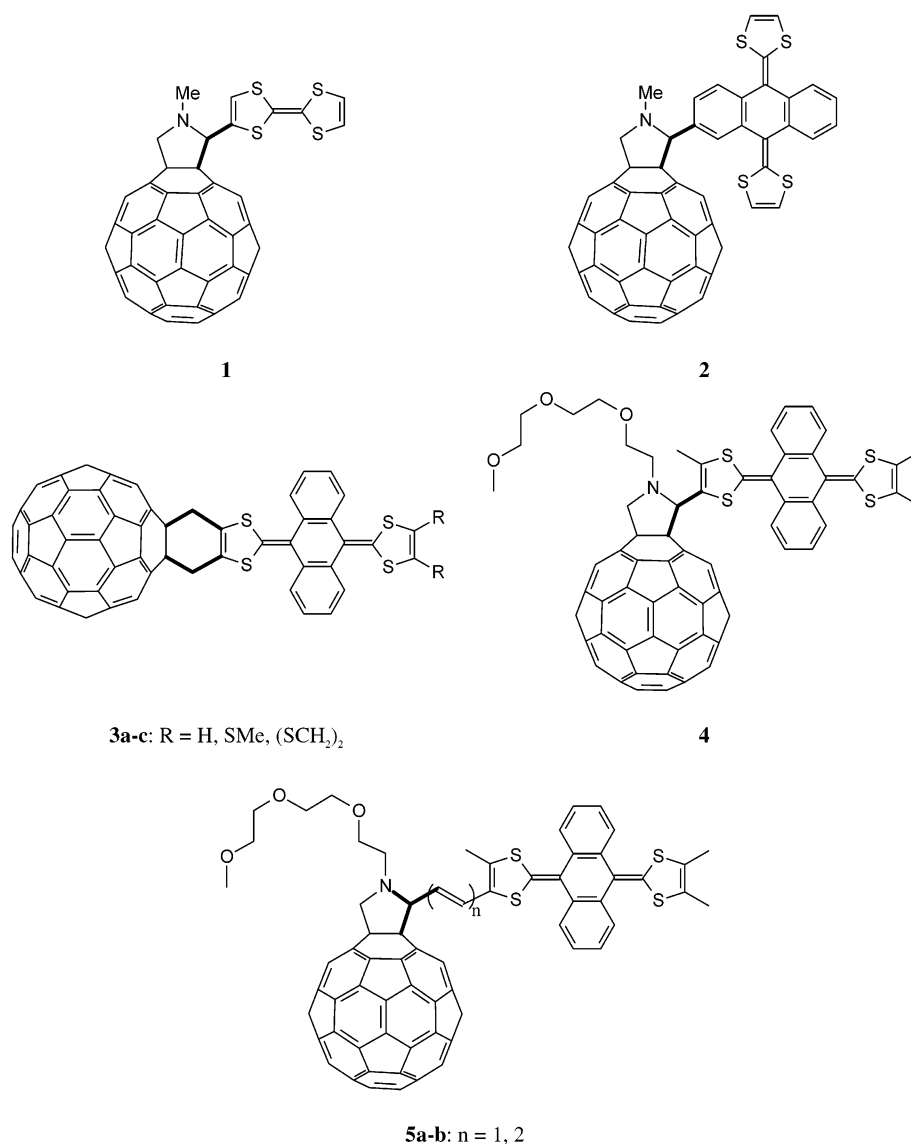
(1) (a) Guldi, D. M., Martín, N., Eds. *Fullerenes: From Synthesis to Optoelectronic Properties*; Kluwer Academic Publishers: Dordrecht, 2002. (b) Prato, M., Martín, N., Eds. Special issue on Functionalized Fullerene Materials. *J. Mater. Chem.* **2002**, *12*, 1931–2159.

(2) Echegoyen, L.; Echegoyen, L. E. *Acc. Chem. Res.* **1998**, *31*, 593.

(3) Guldi, D. M. *Chem. Commun.* **2000**, 321.

(4) (a) Martín, N.; Sánchez, L.; Seoane, C.; Ortí, E.; Viruela, P. M.; Viruela, R. *J. Org. Chem.* **1998**, *63*, 1268. (b) Martín, N.; Sánchez, L.; Seoane, C.; Fernández, C. *Synth. Met.* **1996**, *78*, 137.

CHART 1



(C₆₀-exTTF-exTTF: $\tau \sim 100 \mu\text{s}$) ever reported for intramolecular charge-recombination in donor-acceptor systems that are comparable in composition, donor-acceptor separation, etc.⁸ Very recently, even a transnule, that is, a highly fluorinated fullerene (C₆₀F₁₈) derivative, has been used in the design of a novel multicomponent donor-acceptor array—C₆₀F₁₅-exTTF—which exhibits a 870 ns charge-separated state.⁹ Owing

to the increase in aromaticity and planarity that exTTFs undergo upon oxidation of the buckled neutral state, exTTF derivatives reveal a much stronger propensity for stabilizing charge-separated radical ion pairs (C₆₀-exTTF: $\tau \sim 200 \text{ ns}$), relative to the parent TTF derivatives (C₆₀-TTF: $\tau \sim 2 \text{ ns}$), which transform into aromatic compounds upon oxidation, with little change in conformation.

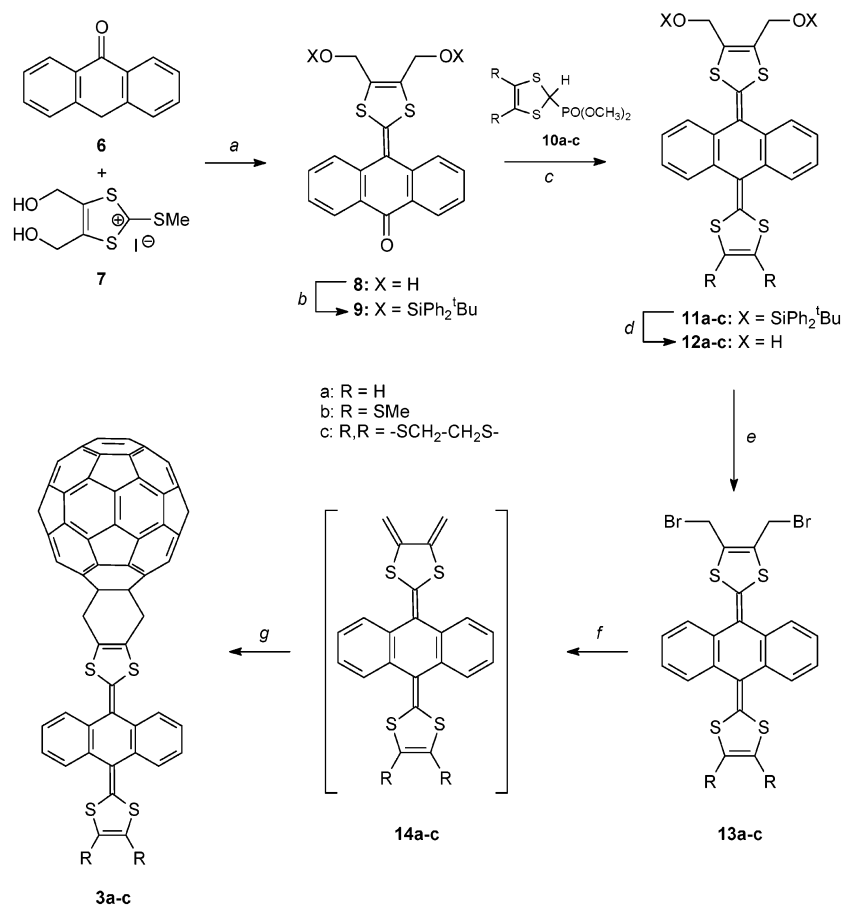
The simplest C₆₀-exTTF dyad (**2**) is depicted in Chart 1, in which the closest 1,3-dithiole ring of the exTTF

(5) (a) Martín, N.; Sánchez, L.; Seoane, C.; Andreu, R.; Garín, J.; Orduna, J. *Tetrahedron Lett.* **1996**, *37*, 5979. (b) Martín, N.; Sánchez, L.; Herranz, M. A.; Guldi, D. M. *J. Phys. Chem. A* **2000**, *104*, 4648. (c) Guldi, D. M.; González, S.; Martín, N.; Antón, A.; Garín, J.; Orduna, J. *J. Org. Chem.* **2000**, *65*, 1978. (d) Martín, N.; Sánchez, L.; Seoane, C.; Andreu, R.; Garín, J.; Orduna, J.; Ortí, E.; Viruela, P. M.; Viruela, R. *J. Phys. Chem. Solids* **1997**, *58*, 1713. (e) Martín, N.; Sánchez, L.; Illescas, B.; González, S.; Herranz, M. A.; Guldi, D. M. *Carbon* **2000**, *38*, 1577. (f) Kreher, D.; Cariou, M.; Liu, S.-G.; Levillain, E.; Veciana, J.; Rovira, C.; Gorgues, A.; Hudhomme, P. *J. Mater. Chem.* **2002**, *12*, 2137 and references therein.

(6) (a) Martín, N.; Pérez, I.; Sánchez, L.; Seoane, C. *J. Org. Chem.* **1997**, *62*, 5690. (b) Martín, N.; Sánchez, L.; Guldi, D. M. *Chem. Commun.* **2000**, 113. (c) Herranz, M. A.; Martín, N.; Sánchez, L.; Seoane, C.; Guldi, D. M. *J. Organomet. Chem.* **2000**, *599*, 2. (d) González, S.; Martín, N.; Swartz, A.; Guldi, D. M. *Org. Lett.* **2003**, *5*, 557.

(7) (a) Sánchez, L.; Pérez, I.; Martín, N.; Guldi, D. M. *Chem. Eur. J.* **2003**, *9*, 2457. (b) Herranz, M. A.; Illescas, B.; Martín, N.; Luo, Ch.; Guldi, D. M. *J. Org. Chem.* **2000**, *65*, 5728. (c) Segura, J. L.; Priego, E. M.; Martín, N. *Tetrahedron Lett.* **2000**, *41*, 7737. (d) Segura, J. L.; Priego, E. M.; Martín, N.; Luo, Ch.; Guldi, D. M. *Org. Lett.* **2000**, *2*, 4121. (e) González, S.; Herranz, M. A.; Illescas, B.; Segura, J. L.; Martín, N. *Synth. Met.* **2001**, *121*, 1131. (f) González, S.; Martín, N.; Guldi, D. M. *J. Org. Chem.* **2003**, *68*, 779. (g) Kodis, G.; Liddell, P. A.; de la Garza, L.; Moore, A. L.; Moore, Th. A.; Gust, D. *J. Mater. Chem.* **2002**, *12*, 2100.

(8) (a) Imahori, H.; Sakata, Y. *Adv. Mater.* **1997**, *9*, 537. (b) Martín, N.; Sánchez, L.; Illescas, B.; Pérez, I. *Chem. Rev.* **1998**, *98*, 2527. (c) Imahori, H.; Sakata, Y. *Eur. J. Org. Chem.* **1999**, 2445, 5. (d) Guldi, D. M.; Maggini, M.; Martín, N.; Prato, M. *Carbon* **2000**, *38*, 1615.

SCHEME 1^a

^a Reagents and conditions: (a) py, AcOH, 70 °C; (b) ^tBuPh₂SiCl/DMF; (c) LDA/THF, -78 °C; (d) Bu₄NF/THF; (e) PBr₃/CCl₄/0 °C; (f) NaI, 18C6; (g) C₆₀/toluene, Δ.

moiety is separated by six bonds from C₆₀. A contrasting pattern is created in the structure of dyad **1**: now only two bonds are placed between the nearest dithiole ring and C₆₀. This topological issue points to a general and sometimes controversially handled question: is the gain of donor aromaticity accountable for the long radical pair lifetimes in dyads of type **2** or, alternatively, is this effect due to larger donor (dithiole ring)–acceptor (C₆₀) separations?

The scope of the current work is to shed light onto this question through molecular tailoring of C₆₀-extendedTTF dyads, such as the newly developed series of (**3a–c**, **4**), in which the 1,3-dithiole ring is connected through two single bonds, similarly to the scenario in dyad **1** and probe them in photophysical experiments. Our strategy involved two basically different connectivities, that is, Diels–Alder cycloaddition and 1,3-dipolar cycloaddition of azomethine ylides to C₆₀. This allowed a comparison of the effect that the connection through one (**4**) or two (**3a–c**) connectivities has on the electron-transfer properties. In addition, we have carried out the synthesis of C₆₀-exTTF dyads (**5a,b**) in which the distance between the dithiole ring and the C₆₀ unit has been systematically increased by adding vinylene units of different length.

(9) Burley, G. A.; Avent, A. G.; Boltalina, O. V.; Goldt, I. V.; Guldi, D. M.; Marcaccio, M.; Paolucci, F.; Paolucci, D.; Taylor, R. *Chem. Commun.* **2003**, 148.

Results and Discussion

Synthesis. The preparation of dyads **3a–c**¹⁰ was carried out in a multistep synthetic procedure from commercially available anthrone (**6**). First, reaction of **6** with dithiolium iodide (**7**)¹¹ produced compound **8** in 54% yield. Forming the bis-hydroxymethyl-substituted exTTFs **12a–c** required protection of the hydroxy groups in **8**, which was done with *tert*-butyldiphenylsilyl chloride in 81% yield. Subsequent Wittig–Horner reaction of **9** with the anion of phosphonate esters **10a–c**¹²—generated in basic medium—led to exTTFs **11a–c**. Finally, exTTFs **11a–c** were reacted with tetrabutylammonium fluoride to give bis-hydroxymethyl exTTFs **12a–c** in 58–93% yields (Scheme 1).

The precursors to dyads **3a–c**—dibromomethyl exTTFs (**13a–c**)—were prepared from **12a–c** by treating them with phosphorus tribromide in THF/CCl₄ at 0 °C. Since **13a–c** undergo iodide-induced 1,4-dehydrohalogenation in the presence of 18-crown-6 to afford “in situ” generated *o*-quinodimethane heteroanalogues,¹³ we trapped them with dienophilic C₆₀. Dyads **3a–c** were obtained as

(10) A preliminary communication reporting dyad **3b** has been previously published. Herranz, M. A.; Martín, N. *Org. Lett.* **1999**, 2005.

(11) Fox, M. A.; Pan, H.-L. *J. Org. Chem.* **1994**, 59, 6519.

(12) (a) Moore, A. J.; Bryce, M. R. *J. Chem. Soc., Perkin Trans. 1* **1991**, 157. (b) Bryce, M. R.; Moore, A. J. *Synthesis* **1991**, 26. (c) Parg, R. P.; Kilburn, J. D.; Ryan, T. G. *Synthesis* **1994**, 195 and references therein.

TABLE 1. Redox Potential Values (± 0.01 V) of Novel Dyads and Related Compounds (V vs SCE)

compd	E^1_{ox} (p a)	E^1_{ox} (p c)	E^1_{red}	E^2_{red}	E^3_{red}
C₆₀^a			-0.60	-1.07	-1.64
3a^a	0.58	-0.04	-0.67	-1.12	-1.72
3b^a	0.68	-0.05	-0.66	-1.17	-1.77
3c^a	0.66	0.12	-0.69	-1.09	-1.67
4^b	0.40	0.12	-0.73	-1.12	-1.67
5a^b	0.44	0.13	-0.71	-1.10	-1.62
5b^b	0.44	0.10	-0.70	-1.09	-1.63
exTTF (18)^c	0.45				
12a^c	0.53	0.02			
12b^c	0.57	0.16			
12c^c	0.57	0.14			
15^c	0.51	0.24	-1.76		
16^c	0.45	-0.22	-1.48		
17^c	0.40	-0.13	-1.36		

^a Experimental conditions: Tol/CH₃CN 4:1 as solvent, GCE as working electrode, Bu₄NClO₄ (0.1 M) as supporting electrolyte; 100 mV s⁻¹. ^b In ODCB/CH₃CN 4:1. ^c In CH₂Cl₂.

yellow-brown solids in 16–34% yields (51–77% based on recovered C₆₀).

The electronic spectra of dyads **3a–c** are dominated, in addition to the typical fullerene bands in the UV region, by absorption bands in the 420–450 nm region, which correspond to the visible transitions of the exTTF moieties. These bands mask, however, the 430 nm absorption band of dihydrofullerenes. In the ¹³C NMR, the quaternary sp³-hybridized carbons, where the organic addends are attached to the C₆₀ sphere, are at around 66 ppm. Furthermore, the number of ¹³C NMR lines observed for C₆₀ derivatives **3a–c** is consistent with a C_{2v} symmetry. The structures were also confirmed by MALDI-TOF mass spectrometry with molecular ions at *m/z* 1126 (**3a**), 1218 (**3b**), and 1216 (**3c**).

Dyads **4** and **5a,b**, on the other hand, were obtained by 1,3-dipolar cycloaddition involving the respective formyl-substituted exTTFs (**15–17**) and C₆₀ in the presence of *N*-substituted glycine.¹⁴ The formyl-containing exTTFs (**16**, **17**) were prepared by Wittig–Horner reaction from formyl-exTTF (**15**)—a product of a previously reported multistep synthetic procedure¹⁵—and phosphoranylideneacetaldehyde to form **16** (81% yield). After a follow-up reaction of **16** with a second molecule of phosphorane, we isolated exTTF **17** in 55% yield. Further reaction of aldehydes **15–17** with *N*-(3,6,9-trioxadecyl)-glycine¹⁶ in refluxing chlorobenzene led to the respective azomethine ylides. In the final step, the in situ generated azomethine ylides undergo 1,3-dipolar cycloaddition to C₆₀ giving dyads **4** and **5a,b** in moderate yields (24–63%) as highly soluble yellow-brown solids (Scheme 2).

Electrochemistry. The redox properties of the novel dyads were studied by cyclic voltammetry at room temperature in a 4:1 toluene/acetonitrile solvent mixture. The data are shown in Table 1 along with those of some of the intermediates (**12a–c** and **15–17**), C₆₀, and the parent π -extended 9,10-bis(1,3-dithiol-2-ylidene)-9,10-dihydroanthracene (**18**).¹⁷

Common to the electrochemical features of all the dyads is the presence of three quasireversible reduction waves, which correspond to the first three reduction steps of the fullerene moiety. As expected, these reduction values are cathodically shifted in comparison with the parent C₆₀, a consequence that stems from saturating a double bond of the C₆₀ core, which raises the LUMO energy. Interestingly, dyads **4** and **5a,b** bearing the trimethyl substituted exTTF donor showed an additional cathodic shift (40–60 mV) of the first reduction potential in comparison to **3a–c**. A possible rationale lies in the electron donor ability of the trimethyl-substituted exTTF unit in **4** and **5a,b**, which is much stronger than those of the exTTF units in dyads **3a–c**. This finding points to electronic interactions between the electroactive units in the ground state, rendering the reduction process in dyads **4** and **5a,b** slightly more difficult.

For the oxidation process, all dyads showed a quasireversible oxidation wave involving a two-electron process to form the dication species.^{6,17} The trimethyl substituted exTTFs in dyads **4** and **5a,b** showed oxidation potentials at values that are positively shifted by 180–280 mV relative to the exTTF units in dyads **3a–c**.¹⁸ The re-reduction process of the exTTF dications back to the neutral molecules is observed in all cases, and occurs with a separation of around 300–600 mV relative to the anodic oxidation peak. The large potential gap between oxidation and re-reduction is indicative of the difficulties that a planar and aromatic dication species experiences by forming a highly distorted neutral molecule.

The redox potentials of intermediate donors **12a–c** and **15–17** have also been included in Table 1. Compounds **12a–c** showed slightly better electron-donor ability than that observed in dyads **3a–c**, which can be accounted for by the electronic effect of the two hydroxymethyl groups as substituents on the 1,3-dithiole ring.

An interesting trend was seen in compounds **15–17** since the proximity of the conjugated formyl group exerts a strong impact on the oxidation of the 1,3-dithiole rings. In particular, compound **15**, in which the carbonyl group is directly linked to the dithiole ring shows a more positive oxidation potential value than **16** ($\Delta E_{\text{ox}} = 60$ mV) bearing a vinylene spacer, and **17** ($\Delta E_{\text{ox}} = 110$ mV) bearing two vinylene units as spacer between the formyl and exTTF moieties (Table 1). Compounds **15–17** present an additional reduction wave at negative values corresponding to the reduction of the carbonyl group which is also influenced by the distance to the 1,3-dithiole ring.

Photophysics. The fullerene fluorescence, although principally weak in nature (i.e., $\sim 6.0 \times 10^{-4}$ for most investigated monoadducts), has been proven to be a sensitive and useful marker for probing excited-state interactions, as they may prevail in C₆₀-based donor–acceptor systems.¹⁹ For instance, connecting an electron donor, such as exTTF, to C₆₀ leads to ensembles in which the fullerene still acts as the primary photosensitizer in

(13) For a review of *o*-quinodimethanes, see: Segura, J. L.; Martín, N. *Chem. Rev.* **1999**, *99*, 3199.

(14) Prato, M.; Maggini, M. *Acc. Chem. Res.* **1998**, *31*, 519.

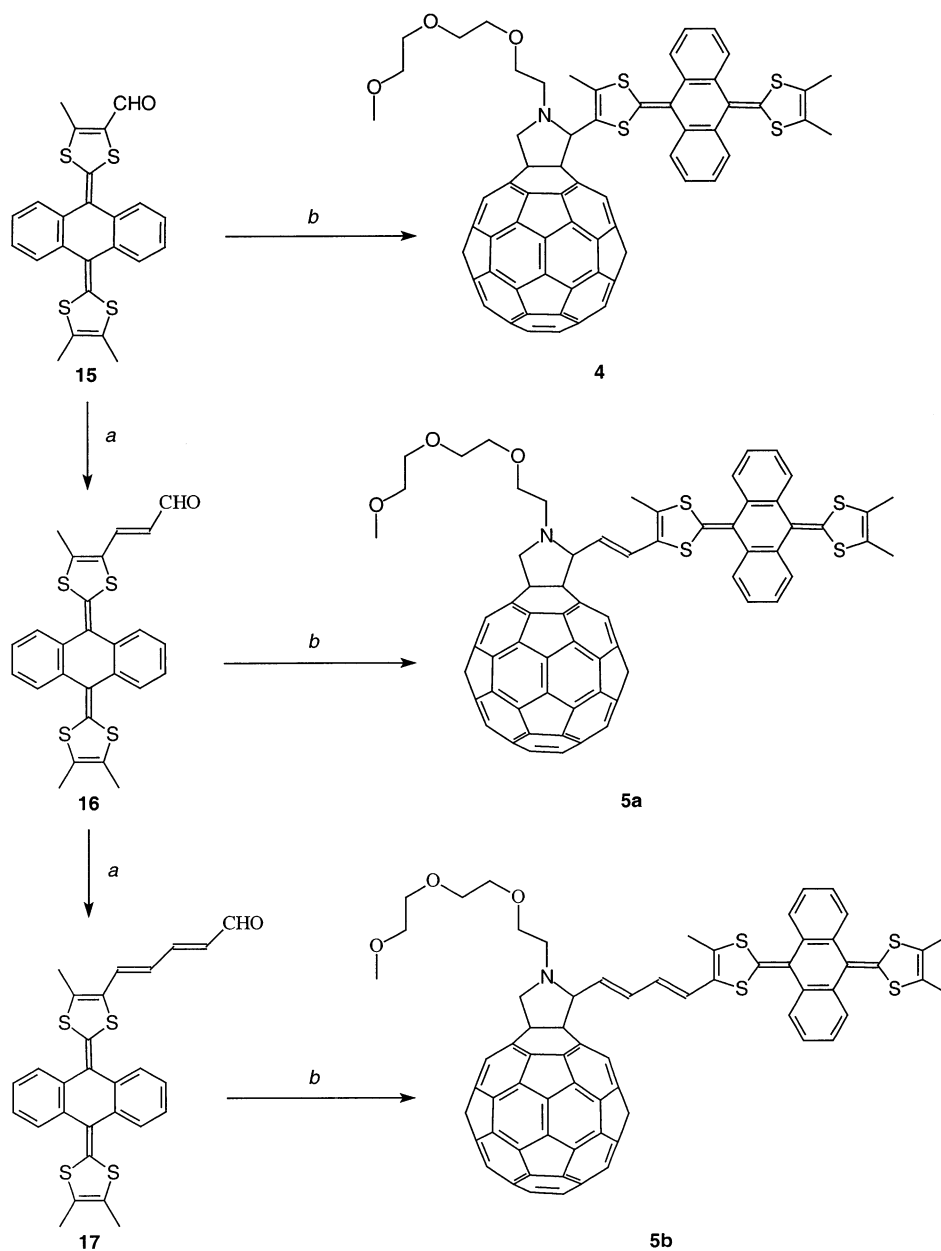
(15) Bryce, M. R.; Finn, T.; Moore, A. J.; Batsanov, A. S.; Howard, J. A. K. *Eur. J. Org. Chem.* **2000**, 51.

(16) Da Ros, T.; Prato, M.; Novello, F.; Maggini, M.; Banfi, E. *J. Org. Chem.* **1996**, *61*, 9070.

(17) (a) Yamashita, Y.; Kobayashi, Y.; Miyashi, T. *Angew. Chem., Int. Ed. Engl.* **1989**, *28*, 1052. (b) Bryce, M. R.; Moore, A. J.; Hasan, M.; Ashwell, G. J.; Fraser, A. T.; Clegg, W.; Hurshouse, M. B.; Karaulov, A. I. *Angew. Chem., Int. Ed. Engl.* **1990**, *29*, 1450.

(18) (a) Farges, J.-P., Ed. *Organic Conductors. Fundamentals and Applications*; Marcel Dekker: New York, 1994. (b) For a recent review on TTFs, see: Segura, J. L.; Martín, N. *Angew. Chem., Int. Ed.* **2001**, *40*, 1372.

(19) Guldi, D. M.; Prato, M. *Acc. Chem. Res.* **2000**, *33*, 695.

SCHEME 2 ^a

^a Reagents and conditions: (a) Ph₃P=CH-CHO, toluene, Δ; (b) C₆₀, CH₃(OCH₂CH₂)₃NHCH₂CO₂H, CIPh, Δ.

the 320–360 nm range. Taking the fullerene's susceptibility toward electrons, especially that of the singlet excited state, and the strong donor properties of exTTF into concert, charge separation is expected to dominate the deactivation of the photoexcited fullerene. One important aspect of the current investigation is to explore the consequence of different functionalization methodologies of the fullerene core, that is, the specific linkage of the exTTF, on the electron-transfer dynamics.

In an effort to characterize the photophysics of C₆₀-exTTF dyads (in **3a–c**, **4**, and **5a,b**) a series of time-resolved and steady-state experiments were conducted in different solvents, ranging from toluene ($\epsilon = 2.38$) to benzonitrile ($\epsilon = 24.8$). In particular, the steady-state fluorescence spectra of **3a–c**, **4**, and **5a,b** in toluene and benzonitrile were probed as a first, crude measure to indicate excited state interactions. The reference, namely

N-methylpyrrolidino[3',4':1,2][60]fullerene itself shows only a weak solvent dependence. Specifically, the *0–0 transition shifts progressively from 713 nm (toluene) to 719 nm (benzonitrile), while the emission intensity remains unaffected.

The picture is, however, fundamentally different for the currently investigated processes in **3a–c**, **4**, and **5a,b**—see Figure 1. Their fluorescence is subject to a strong quenching relative to the corresponding fullerene reference, which is in line with our previous studies on a series of exTTF moieties linked either to a methanofullerene (i.e., [6–6]-closed and [6–5]-open)^{6b} or a fulleropyrrolidine.^{7a} Importantly, the pattern of the fullerene fluorescence with strong *0–0 maxima round 715 nm is fully preserved, despite the overall quenching. A closer inspection of the fluorescence quantum yields (see Tables 2 and 3) reveals several trends in **3a–c** and **4**, **5a,b**

TABLE 2. Photophysical and Thermodynamic Properties of Dyads **3a–c**

	solvent	3a	3b	3c
$-\Delta G_{CS}^{\circ}$	toluene ^b	0.51 eV	0.42 eV	0.41 eV
	bzcn ^b	0.58 eV	0.49 eV	0.48 eV
$-\Delta G_{CR}^{\circ}$	toluene ^a	1.25 eV	1.34 eV	1.35
	bzcn ^b	1.18 eV	1.27 eV	1.28
fluorescence quantum yield (Φ)	toluene	0.68×10^{-4}	1.24×10^{-4}	1.02×10^{-4}
	bzcn	0.25×10^{-4}	0.41×10^{-4}	0.32×10^{-4}
fluorescence quenching $I_0(\text{ref})/I(\text{dyad})$	toluene	8.8	4.8	5.9
	bzcn	24	14.6	18.8
lifetime (τ) C ₆₀ singlet excited state	toluene	0.21 ns	0.31 ns	0.24 ns
	bzcn	0.07 ns	0.12 ns	0.11 ns
lifetime (τ) radical pair	toluene	13 ns	20 ns	12 ns
	bzcn	174 ns	172 ns	167 ns

^a Sum of oxidation and reduction potentials: see Table 1. ^b Determined by eqs 1–3.

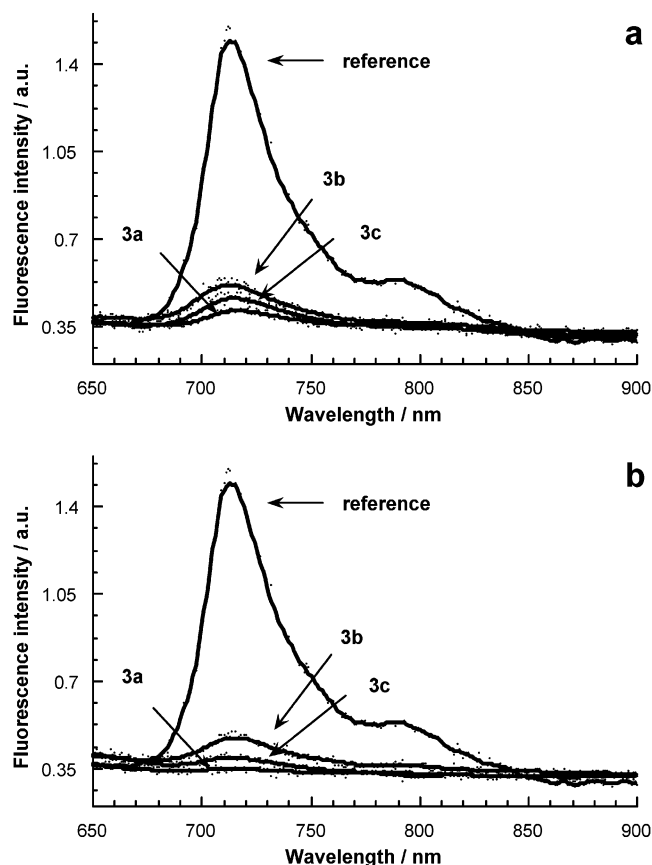


FIGURE 1. Emission spectra of dyads **3a–c** and a *N*-methylpyrrolidino[3',4':1,2][60]fullerene as reference in (a) toluene and (b) in benzonitrile with matching absorption at the 337 nm excitation wavelength (i.e., OD₃₄₀ nm = 0.2).

regarding the magnitude of fluorescence quenching. First, in **3a–c** and **4** the quenching correlates well with the oxidation strength of the exTTF donor. Second, in **3a–c** and **4**, **5a,b** the quenching increases progressively with the solvent polarity. Third, increasing the donor–acceptor separation from **4** to **5a** and **5b** led to a reactivation of the fullerene fluorescence. These findings are in agreement with those previously reported for related structures bearing a ferrocene moiety connected to the C₆₀ core through different vinylene units.²⁰ Extreme scenarios in each series are benzonitrile as a solvent and H- or CH₃-

(20) Guldi, D. M.; Maggini, M.; Scorrano, G.; Prato, M. *J. Am. Chem. Soc.* **1997**, *119*, 974.

substitution on the exTTF donor (**3a**, **4**) yielding fluorescence quantum yields as low as 0.1×10^{-4} . On the contrary the highest values, namely, 1.24×10^{-4} and 1.46×10^{-4} were found in toluene for the $-S-CH_3$ substitution (**3b**) and the donor–acceptor dyad with two vinylene units (**5b**), respectively. A rationalization for these qualitative values infers that the fullerene singlet excited state, as the predominantly populated state, is readily deactivated by an intramolecular electron-transfer event. In the current dyads, it is expected that this evolves from a reaction between the singlet excited state (1.76 eV) of the electron accepting fullerene moiety and the exTTF donor and yields C₆₀^{•-}-exTTF^{•+}.

Probably the most important observation is that the chemical coupling between the donor and acceptor leads to insignificant effects on the quenching at least in the fulleropyrrolidine,^{7a} Diels–Alder adducts,²¹ and **3a–c**. This can be rationalized by reference to the fullerene reduction potentials, which remain virtually unchanged in all these C₆₀ derivatives. A slightly different outline is deduced once we consider the better electron donor features in **4** and **5a,b**, for which the oxidation potential of the donor is around 0.4 eV, appreciably less anodic than those found in **3a–c** (~0.6 eV). The donor strength is known to be one of the central parameters in modulating the energy of charge-separated states and, thereby, impacting the free energy changes for an intramolecular electron transfer. To substantiate this energetic consideration we estimated the driving forces ($-\Delta G_{CR}^{\circ}$ (eV)) (eq 1) for the intramolecular charge-recombination (CR) processes via²²

$$-\Delta G_{CR}^{\circ} = E_{1/2}(D^+/D) - E_{1/2}(A/A^-) + \Delta G_S \quad (1)$$

where $E_{1/2}(D^+/D)$ is the first one-electron oxidation potential of the exTTF donor moiety, while $E_{1/2}(A/A^-)$ refers to the first one-electron reduction potential of the C₆₀ electron acceptor. In the next step, we elucidate the role of the solvent (ΔG_S)²³ on the relative energy of the

(21) Herranz, M. A.; Martín, N.; Ramey, J.; Guldi, D. M. *Chem. Commun.* **2002**, 2968.

(22) (a) Weller, A. *Z. Phys. Chem. (Wiesbaden)* **1982**, *93*, 1982. (b) Imahori, H.; Hagiwara, K.; Aoki, M.; Akiyama, T.; Taniguchi, S.; Okada, T.; Shirakawa, M.; Sakata, Y. *J. Am. Chem. Soc.* **1996**, *118*, 11771. (c) van Dijk, S. I.; Groen, C. P.; Hartl, F.; Brouwer, A.; Verhoeven, J. W. *J. Am. Chem. Soc.* **1996**, *118*, 8425.

(23) Determined from the following relations: R_D = radius donor; R_{D-A} = donor–acceptor separation; R_A = radius acceptor (4.4 Å); ϵ_S = solvent dielectric constant (toluene = 2.39; benzonitrile = 24.8); ϵ_R = solvent dielectric constant for electrochemical measurements (9.412).

TABLE 3. Photophysical and Thermodynamic Properties of Dyads 4, 5a,b

	solvent	4	5a	5b
−ΔG _{CS} ^o	toluene ^b	0.63 eV	0.61 eV	0.62 eV
	bzcn ^b	0.7 eV	0.7 eV	0.73 eV
−ΔG _{CR} ^o	toluene ^a	1.13 eV	1.15 eV	1.14 eV
	bzcn ^b	1.06 eV	1.06 eV	1.03 eV
fluorescence quantum yield (Φ)	toluene	0.16 × 10 ^{−4}	0.62 × 10 ^{−4}	1.46 × 10 ^{−4}
	bzcn	0.1 × 10 ^{−4}	0.1 × 10 ^{−4}	0.65 × 10 ^{−4}
fluorescence quenching I ₀ /I	toluene	37.5	9.7	4.1
	bzcn	60	60	9.2
lifetime (τ) C ₆₀ singlet excited state	toluene	0.19 ns	0.35 ns	0.51 ns
	bzcn	0.08 ns	0.14 ns	0.23 ns
lifetime (τ) radical pair	toluene	21 ns		189 ns
	bzcn	180 ns	725 ns	1465 ns

^a Sum of oxidation and reduction potentials; see Table 1. ^b Determined by eqs 1–3.

charge-separated state by referring to the “dielectric continuum model” (eq 2):

$$\Delta G_S = \frac{e^2}{4\pi\epsilon_0} \left[\left(\frac{1}{2R_+} + \frac{1}{2R_-} - \frac{1}{R_{D-A}} \right) \frac{1}{\epsilon_S} - \left(\frac{1}{2R_+} + \frac{1}{2R_-} \right) \frac{1}{\epsilon_R} \right] \quad (2)$$

Furthermore, the driving forces (−ΔG_{CS}^o (eV)) for the intramolecular charge-separation (CS) processes were determined by eq 3:

$$-\Delta G_{CS}^o = \Delta E_{0-0} - (-\Delta G_{CR}) \quad (3)$$

Hereby, ΔE₀₋₀ is the energy of the 0–0 transition energy gap between the lowest excited state and the ground state (1.76 eV). The accordingly calculated −ΔG_{CS}^o and −ΔG_{CR}^o values are given in Tables 2 and 3. Clearly, the better electron donor in **4** and **5a,b** increases the energy gap between the excited state of the fullerene and the charge-separated state by about 0.2 eV relative to **3a–c**.

Comparable trends were noted in the picosecond transient absorption studies. These experiments were conducted to complement the emission experiments and, more fundamentally, to examine the deactivation dynamics of the photoexcited fullerene core. In addition, this technique enabled us not only to characterize the initially generated state, which is expected to be the fullerene singlet excited state, but also the resulting photoproducts. Thus, to probe the singlet and triplet excited-state behavior of the C₆₀-exTTF dyads, time-resolved differential absorption spectra were recorded immediately following pico- and nanosecond laser excitation. The pump wavelength was alternatively 355 or 337 nm. Specifically, 355 nm illumination of dyads in toluene leads to the instantaneous formation of a new transient absorption, which maximizes around 900 nm. In line with the above assumption, we assign the instantaneously formed transient to the fullerene singlet excited state; see Figure 2.¹⁹ This singlet–singlet absorption decays rapidly with time constants that depend, similar to the fluorescence quenching, on the donor strength (i.e., compare **3a** and **3b**), the solvent polarity, and the donor–acceptor separation (i.e., compare **4** and **5b**). For example, a qualitatively similar picture was noted in polar solvents, such as benzonitrile, with the exception that the singlet excited state deactivation is significantly accel-

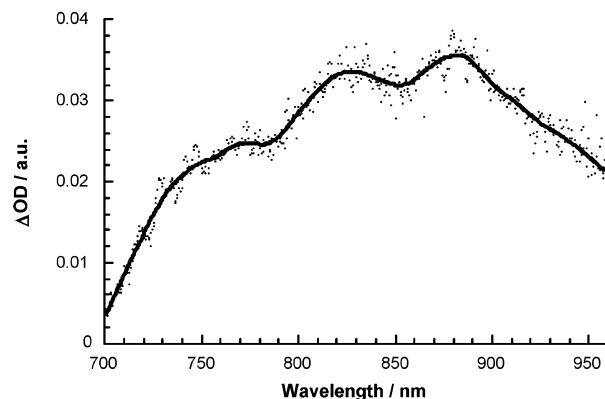


FIGURE 2. Picosecond transient absorption spectrum (visible–near-infrared part) recorded 50 ps (dashed line) and 5000 ps (solid line) upon flash photolysis of dyad **4a** (5.0×10^{-5} M) at 355 nm in deoxygenated benzonitrile, indicating the fullerene singlet–singlet (λ_{\max} at 880 nm).

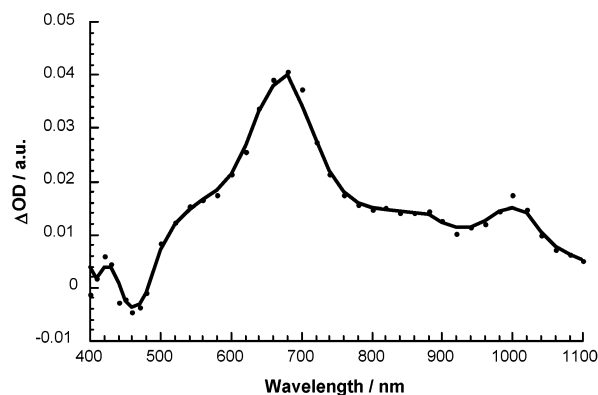


FIGURE 3. Transient absorption spectrum (visible–near-infrared part) recorded 50 ns upon flash photolysis of dyad **4a** (2.0×10^{-5} M) at 337 nm in deoxygenated benzonitrile, indicating the charge-separated radical pair features (λ_{\max} at 680 and 1000 nm).

ated relative to nonpolar toluene. Typically, they range between 500 and 50 ps and, thus, corroborate qualitatively the trend seen in the emission experiments.

At this point, it is worth noting that all the fullerene references, such as methanofullerene, pyrrolidino-fullerene, and triazolinofullerene, disclose after the completion of the initial excitation process a slow, spin-forbidden intersystem crossing affording the energetically lower lying triplet excited state.¹⁹ The absorption decays in the

900 nm region, while a simultaneous grow-in of a new absorption dominates the absorption changes in the 700 nm region, corresponding to the fullerene triplet–triplet absorption. Importantly, none of these new dyads show any appreciable triplet absorption (in the range between 690 and 740 nm).¹⁹ In contrast to the fast rates, seen for the C₆₀-based donor–acceptor systems, the intersystem crossing processes in these references take place on a time scale of 1.8 ns. These quantitatively formed triplet states are characterized by sets of transient absorption bands with maxima around 360 and 700 nm. A clean monoexponential recovery of the singlet ground state follows at low fullerene concentration and low laser power, affording a triplet lifetime of nearly 100 μ s. Employing, however, higher fullerene concentration and/or higher laser power, the kinetics become more complicated: they are impacted primarily by efficient (i) triplet–triplet and (ii) triplet–ground-state annihilation processes. Although substantial, these annihilation processes had, within the applied concentration range ($\leq 5.0 \times 10^{-5}$ M), no significant effect on the fullerene singlet lifetime.

Evidence for the electron-transfer came from time-resolved photolysis studies, namely, as a consequence of the fast singlet decay, the grow-in of a new transient developed in the monitored wavelength range (i.e., 450–960 nm) with maxima at 660 nm (Figure 3).²⁴

The product of electron transfer, namely, the charge-separated radical pair, was unequivocally confirmed by the spectral fingerprints of the one-electron oxidized electron donor– π -radical cation of the exTTF moiety, exTTF^{•+}, and the one electron reduced electron acceptor–fullerene π -radical anion, C₆₀^{•-}. The strongest absorption of the exTTF^{•+} moiety shifted in accordance with the substitution pattern of the donor and covered a range between 650 and 680 nm. Similarly, the absorption of C₆₀^{•-} lies at around 1000 nm. The exact location of these absorption bands was independently confirmed in a set of complementary pulse radiolysis experiments focusing on the radical-induced oxidation and reduction of the exTTF-donor and fullerene-acceptor, respectively.

The strong absorptions of the one-electron reduced fullerenes (C₆₀^{•-}) and of the one-electron oxidized exTTF (exTTF^{•+}) allow an accurate determination of the lifetime of the radical pair; see Tables 2 and 3. An important conclusion in this context is the fact that the charge recombination kinetics are only marginally effected by the type of functionalization, which, in turn, determines the distance separating the donor from the acceptor. Compare, for example, the stabilization of the charge-separated in the pyrrolidinofullerene (~200 ns in benzonitrile)^{7a} and the Diels–Alder adducts (~200 ns in benzonitrile).²¹ These data also confirm the hypothesis that the positive charge, evolving from the intramolecular electron transfer, is delocalized over the entire donor, rather than stabilized on one of the dithiole rings. As a consequence, linking the donor via the anthracene or alternatively via the dithiole moiety has no profound effects on the lifetime of the radical pair. The radical pair lifetime changes, however, substantially when increasing the donor–acceptor distances. In particular, separating the donor in the **4**, **5a,b** series by one or two vinylene

units exerts a profound impact with lifetimes as long as ~1500 ns.

Conclusions

We have carried out the synthesis of two new series of C₆₀-exTTF dyads in which the exTTF donor is connected through one (**4**, **5a,b**) or two (**3a–c**) single bonds by using the 1,3-dipolar cycloaddition reaction of in situ generated azomethine ylides and the Diels–Alder cycloaddition reaction, respectively.

The electrochemical data show the stronger electron donor ability of the trimethyl substituted exTTF in compounds **4**, **5a,b** in comparison with **3a–c** and suggest an electronic interaction between the electroactive units in the ground state. The amphoteric redox behavior of these dyads is confirmed by the reduction waves associated with the fullerene unit which are cathodically shifted in comparison with the parent [60]fullerene.

Fluorescence and time-resolved and steady-state experiments in different solvents were carried out to determine the photophysical behavior of the new compounds (**3a–c**, **4**, **5a,b**). In all cases, the fullerene singlet excited state deactivated rather rapidly via an intramolecular electron transfer process, affording the charge-separated radical pair. The latter which was unequivocally confirmed by the spectral fingerprints of C₆₀^{•-} (1000 nm) and exTTF^{•+} (650–680 nm).

One of the most important conclusions is that the slow recombination kinetics are only marginally effected by the type of functionalization of the C₆₀ moiety and, therefore, the lifetimes determined for the charge separated state are quite similar (~200 ns in benzonitrile) in structurally analogous fulleropyrrolidines and Diels–Alder cycloadducts. These findings confirm that the positive charge of the formed exTTF radical cation is delocalized over the whole donor moiety rather than on one of the two dithiole rings. As a result, the radical pair lifetimes are not significantly influenced by the anthracene or dithiole linkage to the C₆₀ unit.

Experimental Section

General Procedures. 4,5-Bis(hydroxymethyl)-2-(methylthio)-1,3-dithiolium iodide **7**¹¹ and phosphonate esters (**10a–c**)¹² were obtained by previously reported procedures. Aldehyde **15** was obtained by a route different from that reported previously.¹⁵ The corresponding hydroxymethyl derivative²⁵ was treated with selenium dioxide in refluxing THF–dioxane for 15 h, followed by column chromatography on silica with EtOAc/hexane (1:1) as eluent to afford **9** in 51% yield.

9-[4,5-Bis(hydroxymethyl)-1,3-dithiol-2-ylidene]-9,10-dihydroanthracen-10-one (8). To a stirred solution of anthrone **6** (190 mg, 0.98 mmol) in pyridine/acetic acid (44 mL, 3:1) was added 4,5-bis(hydroxymethyl)-2-(methylthio)-1,3-dithiolium iodide (**7**) (340 mg, 1.01 mmol). The resulting deep red solution was heated at 60–70 °C for 16 h. The solvent was then removed under vacuum and the residue extracted with ethyl acetate (2 \times 100 mL). The combined organic extracts were washed with water (2 \times 100 mL) and aqueous sodium bicarbonate 1 M (2 \times 50 mL). After drying over MgSO₄, the solvent was removed under reduced pressure to afford a red solid, which was further purified by column chromatography on silica gel using hexane: ethyl acetate (1:1) to remove the

(24) Guldi, D. M.; Sánchez, L.; Martín, N. *J. Phys. Chem. B* **2001**, *105*, 7139.

(25) Godbert, N.; Bryce, M. R.; Dahanoui, S.; Batsanov, A. S.; Howard, J. A. K.; Hazendonk, P. *Eur. J. Org. Chem.* **2001**, 749.

unreacted anthrone, followed by ethyl acetate to get compound **8**. Additionally, recrystallization from ethyl acetate afforded **8** as thin red needles: 54% yield; mp 261–263 °C (lit. 245–247 °C dec);²⁶ ^1H NMR (DMSO- d_6 , 200 MHz) δ 8.13 (d, 2H, J = 7.8 Hz), 7.94 (d, 2H, J = 7.8 Hz), 7.78 (t, 2H, J = 7.8 Hz), 7.50 (t, 2H, J = 7.8 Hz), 5.59 (t, 2H, J = 5.9 Hz), 4.35 (d, 4H, J = 5.9 Hz); ^{13}C NMR (DMSO- d_6 , 50 MHz) δ 182.0, 156.4, 142.5, 138.3, 132.2, 130.5, 129.4, 126.4, 126.3, 115.5, 56.7; FTIR (KBr) 3217, 2852, 1618, 1587, 1488, 1460, 1437, 1398, 1302, 1244, 1180, 1057, 1034, 1018, 1001, 905, 688 cm^{-1} ; UV-vis (CH_2Cl_2) λ_{max} 472, 366, 274, 254 nm; MS (EI) m/z 354 (M^+). Anal. Calcd for $\text{C}_{19}\text{H}_{14}\text{O}_3\text{S}_2$: C, 64.40; H, 3.99; S, 18.10. Found: C, 64.30; H, 4.33; S, 18.90.

9-[4,5-Bis(*tert*-butyldiphenylsilyloxymethyl)-1,3-dithiol-2-ylidene]-9,10-dihydroanthracene (9). To a solution of **8** (300 mg, 0.85 mmol) in dry DMF (10 mL) was added *tert*-butylchlorodiphenylsilane (0.65 mL, 2.61 mmol) followed by imidazole (1.23 g, 18.1 mmol) and the reaction stirred under argon for 16 h at 20 °C. The crude reaction product was dissolved in ethyl acetate, washed with water, and dried over MgSO_4 . After removal of the solvent in vacuo, column chromatography on silica gel with hexane/dichloromethane (2:1) as eluent afforded compound **9**: 81% yield; mp 118–120 °C dec (lit.²⁶ mp 128–129 °C); ^1H NMR (CDCl_3 , 300 MHz) δ 8.32 (d, 2H, J = 7.8 Hz), 7.94 (d, 2H, J = 8.0 Hz), 7.66 (t, 2H, J = 7.8 Hz), 7.60–7.57 (m, 8H), 7.47–7.26 (m, 14H), 4.20 (s, 4H), 1.02 (s, 18H); ^{13}C NMR (CDCl_3 , 75 MHz) δ 183.6, 151.8, 147.0, 143.8, 139.2, 135.5, 132.4, 131.5, 130.5, 129.9, 129.2, 127.8, 127.0, 126.3, 126.1, 116.7, 59.0, 26.7, 19.2; FTIR (KBr) 2928, 2855, 1961, 1896, 1828, 1643, 1589, 1567, 1486, 1361, 1262, 1113, 940, 821, 771, 609 cm^{-1} ; UV-vis (CH_2Cl_2) λ_{max} 490, 370, 270, 254 nm; MS (FAB^+) m/z 832 (M^+). Anal. Calcd for $\text{C}_{51}\text{H}_{50}\text{O}_3\text{S}_2\text{Si}_2$: C, 73.70; H, 6.10; S, 7.70. Found: C, 73.60; H, 6.30; S, 7.70.

Wittig–Horner Reactions for the Preparation of Donor Systems Derived from Bis(*tert*-butyldiphenylsilane). General Procedure. To a solution of the appropriate phosphonate ester (**10a–c**) (1 mmol) in dry THF (20 mL) at -78 °C and under argon atmosphere was added lithium diisopropyl amide (LDA) (1.1 mmol). After 1 h at -78 °C, a solution of compound **9** in dry THF (150 mg, 0.18 mmol) was added with a syringe. The mixture was stirred for 1 h at -78 °C and then allowed to warm to 20 °C and kept at this temperature overnight. The THF was evaporated under reduced pressure, water (50 mL) added, and the residue extracted with CH_2Cl_2 (3×50 mL). The combined extracts were dried (MgSO_4) and filtered, and the solvent was removed under reduced pressure. Purification of products was achieved by column chromatography on silica gel using hexane/dichloromethane (2:1) as eluent.

9-[4,5-Bis(*tert*-butyldiphenylsilyloxymethyl)-1,3-dithiol-2-ylidene]-10-(1,3-dithiol-2-ylidene)-9,10-dihydroanthracene (11a): 68% yield; mp 112–114 °C; ^1H NMR (CDCl_3 , 300 MHz) δ 7.66–7.64 (m, 4H), 7.55–7.51 (m, 8H), 7.34–7.21 (m, 16H), 6.25 (s, 2H), 4.10 (d, 2H, AB, J_{AB} = 13.0 Hz), 4.07 (d, 2H, AB, J_{AB} = 13.0 Hz), 0.96 (s, 18H); ^{13}C NMR (CDCl_3 , 50 MHz) δ 135.6, 135.4, 135.2, 135.0, 132.7, 129.8, 128.4, 127.7, 125.9, 125.6, 125.3, 124.9, 122.7, 117.1, 59.2, 26.7, 19.2; FTIR (KBr) 2928, 2854, 2710, 1545, 1518, 1458, 1445, 1427, 1362, 1261, 1188, 1113, 1078, 1055, 999, 939, 823, 800, 781, 756, 739, 700, 675, 644, 606 cm^{-1} ; UV-vis (CH_2Cl_2) λ_{max} 436, 368, 270, 244 nm; MS (FAB^+) m/z 917 (M^+). Anal. Calcd for $\text{C}_{54}\text{H}_{52}\text{O}_2\text{S}_4\text{Si}_2$: C, 70.70; H, 5.70; S, 14.00. Found: C, 70.50; H, 5.70; S, 13.90.

9-[4,5-Bis(*tert*-butyldiphenylsilyloxymethyl)-1,3-dithiol-2-ylidene]-10-(4,5-dimethylthio-1,3-dithiol-2-ylidene)-9,10-dihydroanthracene (11b): 73% yield; mp 160–162 °C; ^1H NMR (CDCl_3 , 200 MHz) δ 7.66–7.61 (m, 2H), 7.49–7.48 (m, 12H), 7.31–7.18 (m, 14H), 4.09 (d, 2H, AB, J_{AB} = 13.2 Hz),

4.02 (d, 2H, AB, J_{AB} = 13.2 Hz), 2.31 (s, 6H), 0.92 (s, 18H); ^{13}C NMR (CDCl_3 , 50 MHz) δ 135.5, 135.3, 134.6, 134.2, 132.6, 129.8, 128.4, 127.7, 126.2, 125.8, 125.7, 125.4, 125.3, 59.2, 26.7, 19.2; FTIR (KBr) 2930, 2856, 1527, 1446, 1427, 1113, 1080, 1059, 823, 781, 756, 737, 700, 677, 644, 606 cm^{-1} ; UV-vis (CH_2Cl_2) λ_{max} 440, 370, 272, 246 nm; MS (FAB^+) m/z 1009 (M^+). Anal. Calcd for $\text{C}_{56}\text{H}_{56}\text{O}_2\text{S}_6\text{Si}_2$: C, 66.60; H, 5.60; S, 19.00. Found: C, 65.60; H, 5.72; S, 18.80.

9-[4,5-Bis(*tert*-butyldiphenylsilyloxymethyl)-1,3-dithiol-2-ylidene]-10-(4,5-ethylenedithio-1,3-dithiol-2-ylidene)-9,10-dihydroanthracene (11c): 65% yield; mp 102–104 °C; ^1H NMR (CDCl_3 , 200 MHz) δ 7.72–7.69 (m, 2H), 7.52–7.50 (m, 10H), 7.40–7.27 (m, 16H), 4.17 (d, 2H, AB, J_{AB} = 12.8 Hz), 4.10 (d, 2H, AB, J_{AB} = 12.8 Hz), 3.29 (s, 4H, 4H), 1.01 (s, 18H); ^{13}C NMR (CDCl_3 , 50 MHz) δ 135.2, 134.7, 134.6, 132.7, 132.6, 129.8, 128.4, 128.1, 127.7, 126.3, 125.6, 125.5, 125.3, 125.1, 120.7, 59.1, 29.6, 26.7, 19.2; FTIR (KBr) 2928, 2855, 2359, 1588, 1516, 1474, 1457, 1445, 1427, 1361, 1282, 1187, 1112, 1080, 1006, 941, 823, 780, 755, 739, 701, 675, 644, 622, 606 cm^{-1} ; UV-vis (CH_2Cl_2) λ_{max} 446, 378, 276, 246 nm; MS (FAB^+) m/z 1007 (M^+). Anal. Calcd for $\text{C}_{56}\text{H}_{54}\text{O}_2\text{S}_6\text{Si}_2$: C, 66.80; H, 5.40; S, 19.00. Found: C, 66.50; H, 5.80; S, 19.40.

π -Extended Tetrathiafulvalenes 12a–c. General Procedure. To a solution of the corresponding bis(*tert*-butyldiphenylsilane) derivative previously synthesized (**11a–c**) (0.08 mmol) in dry THF (10 mL) at 20 °C was added tetrabutylammonium fluoride (72 mg, 0.23 mmol) over a period of 10 min. Stirring was continued under argon atmosphere for 16 h. THF was removed in vacuo, the reaction crude was dissolved in dichloromethane, washed with water, dried over MgSO_4 , and solvent was removed under vacuo. Chromatography of the residue on silica gel using hexane/ethyl acetate (1:2) as eluent afforded compounds **12a–c** as yellow solids.

9-[4,5-Bis(hydroxymethyl)-1,3-dithiol-2-ylidene]-10-(1,3-dithiol-2-ylidene)-9,10-dihydroanthracene (12a): 93% yield; mp 252–254 °C; ^1H NMR (DMSO- d_6 , 300 MHz) δ 7.65–7.62 (m, 2H), 7.58–7.55 (m, 2H), 7.35–7.32 (m, 4H), 6.72 (s, 2H), 5.42 (t, 2H, ABX, $J_{\text{AX}} = J_{\text{BX}} = 5.7$ Hz), 4.26 (dd, 2H, ABX, $J_{\text{AB}} = 13.6$ Hz, $J_{\text{BX}} = J_{\text{AX}} = 5.7$ Hz), 4.18 (dd, 2H, ABX, $J_{\text{AB}} = 13.6$ Hz, $J_{\text{AX}} = J_{\text{BX}} = 5.7$ Hz); ^{13}C NMR (DMSO- d_6 , 75 MHz) δ 136.9, 135.1, 134.8, 133.9, 133.5, 129.8, 126.5, 125.6, 125.1, 121.5, 121.1, 118.4, 56.5; FTIR (KBr) 3432, 3064, 2923, 2854, 1617, 1546, 1517, 1455, 1444, 1281, 1171, 1048, 999, 883, 802, 781, 755, 675, 644, 624 cm^{-1} ; UV-vis (CH_2Cl_2) λ_{max} 432, 366, 270, 244 nm; MS (EI) m/z 440 (M^+), 422 ($\text{M}^+ - 18$).

9-[4,5-Bis(hydroxymethyl)-1,3-dithiol-2-ylidene]-10-(4,5-dimethylthio-1,3-dithiol-2-ylidene)-9,10-dihydroanthracene (12b): 79% yield; mp 199–201 °C; ^1H NMR (DMSO- d_6 , 300 MHz) δ 7.61–7.58 (m, 2H), 7.51–7.48 (m, 2H), 7.40–7.36 (m, 4H), 5.43 (t, 2H, ABX, $J_{\text{AX}} = J_{\text{BX}} = 5.8$ Hz), 4.27 (dd, 2H, ABX, $J_{\text{AB}} = 13.7$ Hz, $J_{\text{BX}} = J_{\text{AX}} = 5.8$ Hz), 4.19 (dd, 2H, ABX, $J_{\text{AB}} = 13.7$ Hz, $J_{\text{AX}} = J_{\text{BX}} = 5.8$ Hz), 2.40 (s, 6H); ^{13}C NMR (DMSO- d_6 , 50 MHz) δ 134.4, 134.1, 133.6, 129.6, 129.4, 126.7, 126.2, 125.3, 125.0, 124.8, 123.6, 120.8, 56.0, 18.4; FTIR (KBr) 3421, 2922, 2853, 1528, 1499, 1445, 1385, 1283, 1171, 1049, 999, 947, 858, 779, 756, 675, 644, 625 cm^{-1} ; UV-vis (CH_2Cl_2) λ_{max} 430, 364, 266, 242 nm; MS (EI) m/z 532 (M^+), 514 ($\text{M}^+ - 18$). Anal. Calcd for $\text{C}_{24}\text{H}_{20}\text{O}_2\text{S}_6$: C, 54.10; H, 3.80; S, 36.10. Found: C, 54.50; H, 4.20; S, 36.10.

9-[4,5-Bis(hydroxymethyl)-1,3-dithiol-2-ylidene]-10-(4,5-ethylenedithio-1,3-dithiol-2-ylidene)-9,10-dihydroanthracene (12c): 58% yield; mp 192–194 °C; ^1H NMR (DMSO- d_6 , 300 MHz) δ 7.60 (m, 2H), 7.43–7.36 (m, 6H), 5.44 (t, 2H, ABX, $J_{\text{AX}} = J_{\text{BX}} = 5.7$ Hz), 4.27 (dd, 2H, ABX, $J_{\text{AB}} = 13.6$ Hz, $J_{\text{BX}} = J_{\text{AX}} = 5.7$ Hz), 4.18 (dd, 2H, ABX, $J_{\text{AB}} = 13.7$ Hz, $J_{\text{BX}} = J_{\text{AX}} = 5.7$ Hz), 3.30 (s, 4H); ^{13}C NMR (DMSO- d_6 , 50 MHz) δ 134.3, 133.6, 129.4, 128.8, 128.1, 127.6, 126.8, 126.2, 125.3, 124.5, 120.6, 110.2, 56.0, 29.1; FTIR (KBr) 3382, 2919, 2850, 1596, 1514, 1456, 1445, 1373, 1281, 1240, 1170, 1048, 1019, 858, 780, 755, 720, 675, 643, 622, 455 cm^{-1} ; UV-vis (CH_2Cl_2) λ_{max} 440, 374, 270, 244 nm; MS (EI) m/z 530 (M^+), 514 ($\text{M}^+ -$

(26) Christensen, C. A.; Bryce, M. R.; Batsanov, A. S.; Becher, J. *Org. Biomol. Chem.* **2003**, *1*, 511.

18). Anal. Calcd for $C_{24}H_{18}O_2S_6$: C, 54.30; H, 3.40; S, 36.20. Found: C, 54.90; H, 4.10; S, 35.90.

π -Extended Tetrathiafulvalenes 13a–c. General Procedure. To a solution of the appropriate bis(hydroxymethyl) derivative **12a–c** (0.05 mmol) in dry THF (1 mL), under argon, and at 0 °C was added carbon tetrachloride (1 mL). While the mixture was stirred, phosphorus tribromide (0.01 mL, 0.07 mmol) was added slowly, and the reaction mixture was kept under these conditions for 1 h. The reaction crude was poured into ethyl acetate (50 mL) and washed with brine. The organic layer was dried over $MgSO_4$, and evaporation of the solvent (below 40 °C) gave an oily orange residue, which was chromatographed using silica gel and a mixture of hexane/ethyl acetate (5:1) as the eluent.

9-[4,5-Bis(bromomethyl)-1,3-dithiol-2-ylidene]-10-(1,3-dithiol-2-ylidene)-9,10-dihydroanthracene (13a): 54% yield; mp > 300 °C; 1H NMR ($CDCl_3$, 300 MHz) δ 7.74–7.71 (m, 2H), 7.60–7.58 (m, 2H), 7.33–7.30 (m, 4H), 6.30 (s, 2H), 4.18 (s, 4H); ^{13}C NMR ($CDCl_3$, 75 MHz) δ 135.4, 134.5, 133.5, 129.1, 128.4, 126.4, 126.0, 125.1, 123.9, 121.6, 117.2, 22.1; FTIR (KBr) 2924, 2853, 2633, 1593, 1560, 1545, 1508, 1445, 1205, 756, 675, 644 cm^{-1} ; UV–vis (CH_2Cl_2) λ_{max} 420, 354, 268, 234 nm; MS (EI) m/z 566 (M^+), 486 ($M^+ - 80$), 406 ($M^+ - 160$). Anal. Calcd for $C_{22}H_{14}S_4Br_2$: C, 46.60; H, 2.50; S, 22.60. Found: C, 47.60; H, 3.10; S, 21.60.

9-[4,5-Bis(bromomethyl)-1,3-dithiol-2-ylidene]-10-(4,5-dimethylthio-1,3-dithiol-2-ylidene)-9,10-dihydroanthracene (13b): 71% yield; mp > 300 °C; 1H NMR ($DMSO-d_6$, 300 MHz) δ 7.58–7.54 (m, 4H), 7.44–7.40 (m, 4H), 4.70 (s, 4H), 2.38 (s, 6H); ^{13}C NMR ($CDCl_3$, 75 MHz) δ 134.6, 134.5, 129.2, 129.0, 126.5, 126.3, 125.8, 125.5, 125.2, 123.5, 123.4, 22.1, 19.2; FTIR (KBr) 2852, 1593, 1526, 1497, 1458, 1445, 1431, 1201, 1024, 779, 754, 675, 642 cm^{-1} ; UV–vis (CH_2Cl_2) λ_{max} 432, 364, 276, 246 nm; MS (EI) m/z 578 ($M^+ - 80$), 498 ($M^+ - 160$). Anal. Calcd for $C_{24}H_{18}S_6Br_2$: C, 43.80; H, 2.75; S, 29.20. Found: C, 44.90; H, 2.95; S, 28.10.

9-[4,5-Bis(bromomethyl)-1,3-dithiol-2-ylidene]-10-(4,5-ethylenedithio-1,3-dithiol-2-ylidene)-9,10-dihydroanthracene (13c): 87% yield; mp > 300 °C; 1H NMR ($CDCl_3$, 200 MHz) δ 7.62–7.58 (m, 2H), 7.55–7.51 (m, 2H), 7.37–7.31 (m, 4H), 4.19 (s, 4H), 3.30 (s, 4H); ^{13}C NMR ($CDCl_3$, 75 MHz) δ 134.6, 134.5, 132.4, 130.0, 129.5, 129.1, 128.3, 126.4, 125.7, 125.2, 123.5, 110.8, 29.6, 22.0; FTIR (KBr) 2921, 2851, 1653, 1594, 1515, 1456, 1445, 1282, 1262, 1201, 1148, 1102, 1056, 939, 919, 886, 857, 801, 779, 756, 703, 675, 643, 620, 597 cm^{-1} ; UV–vis (CH_2Cl_2) λ_{max} 438, 370, 280, 242 nm; MS (EI) m/z 496 ($M^+ - 160$). Anal. Calcd for $C_{24}H_{16}S_6Br_2$: C, 43.90; H, 2.46; S, 29.30. Found: C, 44.80; H, 2.68; S, 28.70.

Diels–Alder Cycloadducts 3a–c. General Procedure. To a refluxing solution of [60]fullerene (50 mg, 0.07 mmol), sodium iodide (47 mg, 0.31 mmol), and 18-crown-6 (55 mg, 0.21 mmol) in toluene (50 mL) was added dropwise a solution of the respective bis(bromomethyl) derivative (**13a–c**) (0.08 mmol) in toluene (5 mL). The resulting green reaction mixture was refluxed for a variable period of time (from 30 min to 2 h). The solvent was removed under vacuo, and the residue was chromatographed on silica gel using cyclohexane/toluene as eluent. Further purification was accomplished by washing the obtained solid three times with hexane, methanol, and diethyl ether, respectively.

Cycloadduct of 9-[4,5-bis(bromomethyl)-1,3-dithiol-2-ylidene]-10-(1,3-dithiol-2-ylidene)-9,10-dihydroanthracene and C_{60} (3a): 34% yield (77% based on recovered C_{60}); 1H NMR ($CDCl_3$, 300 MHz) δ 7.78–7.75 (m, 2H), 7.72–7.69 (m, 2H), 7.33–7.30 (m, 4H), 6.34 (s, 2H), 4.35 (d, 2H, AB, $J_{AB} = 13.3$ Hz), 4.31 (d, 2H, AB, $J_{AB} = 13.3$ Hz); ^{13}C NMR ($CDCl_3/CS_2$ 1/1, 75 MHz) δ 155.2, 154.8, 147.5, 146.4, 146.1, 145.6, 145.4, 145.3, 144.8, 144.7, 144.5, 142.9, 142.4, 142.1, 141.9, 141.5, 140.0, 136.5, 135.7, 135.6, 135.3, 134.9, 134.3, 126.3, 126.1, 125.9, 125.0, 124.9, 122.9, 121.9, 117.2, 65.7, 40.3; FTIR (KBr) 2920, 1573, 1542, 1514, 1456, 1443, 1281, 1259, 1214, 1187, 1161, 1095, 944, 857, 801, 777, 767, 753, 697, 674,

643, 604, 588, 574, 552, 526 cm^{-1} ; UV–vis (CH_2Cl_2) λ_{max} 436, 422, 370, 328, 258 nm; MS (MALDI-TOF) m/z 1126 (M^+), 406 (diene).

Cycloadduct of 9-[4,5-bis(bromomethyl)-1,3-dithiol-2-ylidene]-10-(4,5-dimethylthio-1,3-dithiol-2-ylidene)-9,10-dihydroanthracene and C_{60} (3b): 25% yield (57% based on recovered C_{60}); 1H NMR ($CDCl_3$, 300 MHz) δ 7.84–7.79 (m, 2H); 7.57–7.54 (m, 2H), 7.38–7.29 (m, 4H), 4.37 (d, 2H, AB, $J_{AB} = 14.8$ Hz), 4.33 (d, 2H, AB, $J_{AB} = 14.8$ Hz), 2.43 (s, 6H); ^{13}C NMR ($CDCl_3/CS_2$ 1/1, 75 MHz) δ 155.8, 155.5, 155.1, 148.2, 147.1, 146.8, 146.2, 146.1, 146.0, 145.4, 145.2, 143.6, 143.2, 142.8, 142.6, 142.2, 140.7, 136.4, 136.3, 135.6, 135.2, 131.3, 129.5, 128.7, 128.0, 127.1, 126.9, 126.8, 126.3, 126.0, 125.7, 124.4, 66.4, 41.1, 19.7; FTIR (KBr) 2915, 1522, 1496, 1443, 1426, 1281, 1182, 968, 766, 753, 696, 674, 642, 623, 575, 553, 526 cm^{-1} ; UV–vis (CH_2Cl_2) λ_{max} 442, 424, 316, 260 nm; MS (MALDI-TOF) m/z 1218 (M^+), 498 (diene).

Cycloadduct of 9-[4,5-bis(bromomethyl)-1,3-dithiol-2-ylidene]-10-(4,5-ethylenedithio-1,3-dithiol-2-ylidene)-9,10-dihydroanthracene and C_{60} (3c): 16% yield (51% based on recovered C_{60}); 1H NMR ($CDCl_3$, 300 MHz) δ 7.84–7.81 (m, 2H), 7.61–7.56 (m, 2H), 7.40–7.34 (m, 4H), 4.32 (d, 2H, AB, $J_{AB} = 13.9$ Hz), 4.30 (d, 2H, AB, $J_{AB} = 13.9$ Hz), 3.35–3.33 (m, 4H); ^{13}C NMR ($CDCl_3/CS_2$ 1/1, 75 MHz) δ 155.3, 154.9, 147.5, 146.4, 146.1, 145.6, 145.5, 145.4, 145.3, 144.9, 144.8, 144.6, 144.5, 143.0, 142.9, 142.5, 142.1, 141.9, 141.5, 140.1, 135.8, 135.7, 135.1, 135.0, 134.6, 128.1, 126.4, 126.3, 126.1, 125.5, 125.1, 123.8, 122.6, 65.7, 40.4, 29.7; FTIR (KBr) 2918, 2844, 1507, 1444, 1281, 1261, 1212, 1187, 1095, 1021, 802, 766, 753, 697, 673, 642, 622, 574, 554, 526 cm^{-1} ; UV–vis (CH_2Cl_2) λ_{max} 448, 388, 316, 260 nm; MS (MALDI-TOF) m/z 1216 (M^+), 496 (diene).

Compounds 16 and 17. General Procedure. To a stirred solution of (triphenylphosphoranylidene)acetaldehyde (1 mmol) in dry toluene (20 mL) and under argon atmosphere was added the corresponding aldehyde (**15**, **16**) (0.5 mmol). The mixture was refluxed for 12 h and then allowed to reach 20 °C. Hexane (30 mL) was added, and the triphenylphosphine oxide precipitated was separated by filtration. The solvent was evaporated under vacuum, and the pure product was chromatographed on a silica gel column using hexane/ CH_2Cl_2 in the proportion indicated below as eluent.

9-[4-(2-Formylvinyl)-5-methyl-1,3-dithiol-2-ylidene]-10-(4,5-dimethyl-1,3-dithiol-2-ylidene)-9,10-dihydroanthracene (16): hexane/ CH_2Cl_2 (1:1); 81% yield; mp 252 °C; 1H NMR ($CDCl_3$, 200 MHz) δ 9.57 (d, 1H, $J = 7.3$ Hz), 7.70–7.57 (m, 4H), 7.35–7.30 (m, 4H), 6.75 (d, 1H, $J = 15.6$ Hz), 5.99 (dd, 1H, $J_1 = 15.6$ Hz, $J_2 = 7.3$ Hz) 2.22 (s, 3H), 1.93 (s, 6H); ^{13}C NMR ($CDCl_3$, 75 MHz) δ 191.6, 135.2, 134.9, 134.4, 130.4, 129.8, 129.5, 125.9, 125.7, 125.3, 125.2, 120.8, 120.0; FTIR (KBr) 2924, 2852, 1676, 1595, 1560, 1132, 756, cm^{-1} ; UV–vis (CH_2Cl_2) λ_{max} 441, 309, 257 nm; MS m/z 476 (M^+).

9-[4-(4-Formyl-1,3-butadienyl)-5-methyl-1,3-dithiol-2-ylidene]-10-(4,5-dimethyl-1,3-dithiol-2-ylidene)-9,10-dihydroanthracene (17): Hexane/ CH_2Cl_2 (1:4); 55% yield; mp 197 °C; 1H NMR ($CDCl_3$, 300 MHz) δ 9.52 (d, 1H, $J = 7.1$ Hz), 7.68–7.54 (m, 4H), 7.28–7.22 (m, 4H), 7.08–7.03 (m, 1H), 6.72–6.39 (m, 2H), 6.15 (dd, 1H, $J_1 = 15.0$ Hz, $J_2 = 7.1$ Hz) 2.06 (s, 3H), 1.87 (s, 6H); ^{13}C NMR ($CDCl_3$, 75 MHz) δ 191.8, 135.4, 135.1, 134.6, 133.6, 131.5, 130.6, 130.0, 129.7, 128.7, 126.2, 126.1, 125.9, 125.5, 125.4, 125.3, 124.9, 122.7, 120.9, 13.6, 13.2; FTIR (KBr) 2922, 2852, 2331, 1676, 1654, 1558, 1521, 1458, 1155 cm^{-1} ; UV–vis (CH_2Cl_2) λ_{max} 441, 309, 257 nm; MS m/z 502 (M^+).

Fulleropyrrolidines (4, 5a,b). General Procedure. To a solution of C_{60} (0.5 mmol) in chlorobenzene (100 mL) were added *N*-(3,6,9-trioxadecyl)glycine (1.5 mmol) and the corresponding formyl-exTTF derivative **15–17** (0.5 mmol). The mixture was refluxed for 16 h under argon atmosphere. The solvent was partially removed under reduced pressure and was then loaded on a silica gel column, using toluene/ethyl acetate (9:1) as eluent. Further purification was accomplished by

repetitive precipitation and centrifugation with methanol and diethyl ether as solvents.

4: 63% yield (78% based on recovered C_{60}); ^1H NMR (CS_2 , 300 MHz) δ 7.60 (m, 4H), 7.21 (m, 4H), 5.31 (s, 1H), 5.17 (d, 1H, $J = 10.0$ Hz), 4.21 (d, 1H, $J = 10.0$ Hz), 3.90–3.15 (m, 15H), 2.24 (s, 3H), 2.00 (s, 6H); ^{13}C NMR ($\text{CDCl}_3/\text{CS}_2$ 1/1, 125 MHz) δ 155.67, 155.43, 152.97, 152.73, 147.16, 146.21, 146.05, 145.85, 145.72, 145.48, 145.42, 145.34, 145.30, 145.18, 145.17, 145.10, 144.70, 144.23, 142.91, 142.84, 142.63, 142.59, 142.52, 142.24, 142.06, 141.74, 141.61, 141.46, 140.25, 140.11, 139.82, 136.78, 135.14, 134.72, 133.93, 133.20, 127.80, 127.46, 125.94, 125.74, 125.55, 125.48, 125.29, 125.20, 125.04, 124.97, 121.93, 121.69, 121.61, 121.54, 121.07, 120.99, 120.89, 120.83, 75.90, 75.77, 72.18, 71.01, 70.80, 70.69, 67.59, 65.18, 58.61, 52.83, 14.87, 14.67, 13.27; FTIR (KBr) 2912, 2856, 2807, 1619, 1510, 1442, 1384, 1114, 1037, 752, 643, 527 cm^{-1} ; UV-vis (CHCl_3) λ_{max} 441, 309, 257 nm; MS m/z 1329 (M^+).

5a: 24% yield (37% based on recovered C_{60}); ^1H NMR ($\text{CDCl}_3/\text{CS}_2$ 1/1, 300 MHz) δ 7.57 (m, 4H), 7.24 (m, 4H), 6.86 (d, 1H, $J = 15$ Hz), 6.49–6.63 (m, 1H), 6.05–6.95 (m, 1H), 5.09 (d, 1H, $J = 9.8$ Hz), 4.59 (d, 1H, $J = 9.8$ Hz), 4.19–2.90 (m, 16H), 2.14 (s, 3H), 1.98 (s, 3H), 1.91 (s, 3H); ^{13}C NMR ($\text{CDCl}_3/\text{CS}_2$ 1/1, 125 MHz) δ 156.36, 154.68, 153.76, 152.64, 152.46, 147.59, 147.34, 147.07, 146.70, 146.52, 146.42, 146.24, 145.88, 145.54, 145.09, 144.74, 143.52, 143.40, 143.03, 142.96, 142.69, 142.43, 142.05, 140.71, 140.56, 140.46, 140.28, 138.05, 137.83, 137.00, 136.89, 136.36, 136.29, 136.13, 135.92, 135.72, 135.66, 135.52, 135.26, 135.14, 134.74, 134.63, 132.82, 132.72, 131.31, 130.60, 130.49, 130.44, 129.48, 126.63, 126.47, 126.24, 126.13, 126.06, 125.78, 125.66, 125.58, 125.31, 125.22, 125.15, 123.44, 123.13, 122.87, 121.45, 121.35, 121.29, 121.09, 120.94, 120.71, 81.46, 81.13, 75.97, 72.66, 71.46, 71.33, 71.24, 69.85, 67.91, 59.07, 53.13, 13.92, 13.66; FTIR (KBr) 2912, 2864, 1630, 1519, 1443, 1109, 754, 527 cm^{-1} ; UV-vis (CHCl_3) λ_{max} 433, 257, 247 nm; MS m/z 1356 (M^+).

5b: 14% yield (23% based on recovered C_{60}); ^1H NMR (CS_2 , 300 MHz) δ 7.79–7.75 (m, 4H), 7.44–7.34 (m, 4H), 7.00–6.95 (m, 1H), 6.69–6.39 (m, 3H), 5.34 (d, 1H, $J = 9.3$ Hz), 4.85 (d, 1H, $J = 8.9$ Hz), 4.42 (d, 1H, $J = 8.9$ Hz), 4.23–3.19 (m, 15H), 2.39 (s, 3H), 2.26 (s, 3H), 2.22 (s, 3H); ^{13}C NMR ($\text{CDCl}_3/\text{CS}_2$ 1/1, 125 MHz) δ 156.53, 154.74, 153.92, 152.98, 147.58, 147.37, 147.14, 147.08, 146.68, 146.51, 146.41, 146.27, 146.19, 145.92, 145.87, 145.70, 145.63, 145.53, 145.09, 145.04, 144.74, 143.53, 143.39, 143.04, 142.95, 142.69, 142.61, 142.53, 142.41, 142.06, 140.58, 140.46, 137.83, 137.76, 136.89, 136.47, 136.32, 136.13, 135.94, 135.68, 135.27, 134.76, 134.64, 134.44, 132.81, 132.72, 132.29, 131.84, 131.68, 130.61, 130.44, 128.79, 128.75, 126.46, 126.24, 126.19, 126.13, 125.76, 125.68, 125.58, 123.12, 122.88, 122.88, 122.80, 122.75, 121.34, 120.95, 120.83, 81.22, 81.13, 76.11, 72.65, 71.46, 71.32, 71.23, 69.92, 67.91, 59.06, 53.13, 13.87, 13.65; FTIR (KBr) 2961, 2920, 2851, 1636, 1444, 1261, 1097, 1023, 803, 527 cm^{-1} ; UV-vis (CHCl_3) λ_{max} 432, 256, 245 nm; MS m/z 1382 (M^+).

Acknowledgment. This work has been supported by the MCYT of Spain (Project BQU2002-00855). Part of this work was supported by the Office of Basic Energy Sciences of the U.S. Department of Energy (Contribution No. NDRL-4478 from the Notre Dame Radiation Laboratory). The work in Durham was funded by the University of Durham (studentship to N.G.) and Durham County Council under the Science and Technology for Business and Enterprise Program SP/082.

Supporting Information Available: Emission Spectra of dyads **4**, **5a**, and **5b** in toluene, *o*-dichlorobenzene, and benzonitrile. This material is available free of charge via the Internet at <http://pubs.acs.org>.

JO034432E